Available online at www.sciencedirect.com
SCIENCE DIRECT®
ELSEVIER
Earth and Planetary Science Letters 213 (2003) 375–390
EPSL
www.elsevier.com/locate/epsl

# Micromagnetic modeling of first-order reversal curve (FORC) diagrams for single-domain and pseudo-single-domain magnetite

Claire Carvallo [a,*], Adrian R. Muxworthy [a,b], David J. Dunlop [a], Wyn Williams [b]

[a] *Geophysics, Physics Department, University of Toronto at Mississauga, Mississauga, ON, Canada L5L1C6*
[b] *School of GeoSciences, University of Edinburgh, King's Buildings, West Mains Road, Edinburgh EH9 3JW, UK*

Received 31 October 2002; received in revised form 29 May 2003; accepted 30 May 2003

**Abstract**

First-order reversal curve (FORC) diagrams have been experimentally shown to be a better way of discriminating domain states in a sample compared to the straightforward use of major hysteresis loops. In order to better understand the fundamental behavior of assemblages of single-domain (SD) grains, we used a micromagnetic model with a conjugate gradient algorithm to calculate FORC diagrams for isolated grains of magnetite as well as for arrays of grains. In the case of individual elongated grains, we found that the FORC diagram consists of a single peak centered on the coercive force $H_c$ if the grain is SD. For a pseudo-single-domain (PSD) grain with vortex structure, we observe multiple peaks on the FORC diagram. The modeling of arrays of elongated SD particles reveals two distinct types of patterns depending on the spacing between particles. In a $2\times2\times2$ array of particles, a secondary branch on the reversal curves appears if the spacing between particles is less than about twice the particle length. This feature translates into the appearance of one negative and three positive peaks on the FORC diagram. In the case of a $3\times3\times3$ array of particles, we again observe several secondary branches when the spacing between grains is less than about twice the particle length, leading to the appearance of multiple peaks on the FORC diagram. Splitting of the central peak on the $H_u$ axis when particles interact could explain the vertical spread of FORC distributions of natural interacting samples as an effect of superposition of multiple peaks caused by the random orientation and distributions of particle spacing and switching fields of a large number of grains. The presence of symmetric peaks on a FORC diagram can be an indicator of the presence of either small PSD grains or magnetic interactions in an ensemble of grains.


*Keywords:* FORC diagram; interactions; micromagnetic model; magnetic hysteresis; PSD magnetite

## 1. Introduction

The magnetic properties of natural samples are governed by the composition, the grain-size distribution and the interactions among the magnetic

* Corresponding author.
*E-mail address:* carvallo@physics.utoronto.ca (C. Carvallo).

0012-821X/03/$ – see front matter © 2003 Elsevier B.V. All rights reserved.
doi:10.1016/S0012-821X(03)00320-0

particles within the sample. Domain state and composition of magnetic minerals need to be accurately characterized when studying natural magnetic systems in paleomagnetic, environmental and paleoclimatic studies [1]. For instance, the reliability of magnetic recording in rocks, which is critical for paleomagnetism, depends on mineralogical parameters such as the grain size and the composition of the assemblage that carries the magnetic signal. Single-domain (SD) particles (less than 0.07 μm in magnetite [2]) are the most reliable recorders of natural remanent magnetization. They also constitute the ideal material for paleomagnetism and paleofield intensity determination by the Thellier–Thellier method [3]. Pseudo-single-domain (PSD) grains (in the size range between 0.07 and ~10 μm) still carry a stable remanence and behave almost ideally in Thellier–Thellier paleointensity experiments. Multidomain (MD) grains carry the least stable remanence and are the least useful for paleointensity determinations [4].

Magnetostatic interactions in SD assemblies strongly reduce the intensity of thermoremanent magnetization [5]. Interaction among particles is another factor that leads to the failure of paleointensity experiments because the three Thellier laws of partial thermoremanent magnetization (reciprocity, independence and additivity) are violated in the presence of an interaction field. Therefore, it is important to be able to determine both the particle size and the magnetic interaction state in a natural assemblage.

Magnetic grain size is usually determined by measuring the ratio of the saturation remanent magnetization $M_{rs}$ over the saturation magnetization $M_s$ and the ratio of the remanent coercive field $H_{cr}$ over the coercive field $H_c$. Day et al. [6] showed that these parameters plot in different regions on a diagram of $M_{rs}/M_s$ versus $H_{cr}/H_c$ depending on the grain size. However, interpretation of these hysteresis parameters can be ambiguous [7,8]. Interactions are also difficult to detect in a bulk sample. The Henkel plot [9], which compares isothermal remanent magnetization and direct current demagnetization, cannot discriminate between a MD system or an interacting SD system if the mean grain interaction field is negative [10].

First-order reversal curve (FORC) diagrams, introduced in rock magnetism by Roberts et al. [11], provide a new way of identifying minerals and domain states by measuring partial hysteresis curves. The measurement of a FORC diagram begins by magnetically saturating the sample. The field is then decreased to a field $-H_a$ and increased again up to saturation through field steps $H_b$. This process is repeated for about 100 different values of $H_a$. The FORC distribution is defined by [11]:

$$\rho(H_a, H_b) = \frac{\partial^2 M(H_a, H_b)}{\partial H_a \partial H_b} \quad (1)$$

where $M(H_a,H_b)$ is the magnetization measured at $(H_a,H_b)$. A FORC diagram is a contour plot of $\rho(H_a,H_b)$ along axes

$$\left(H_c = \frac{H_b - H_a}{2}, H_u = \frac{H_b + H_a}{2}\right)$$

The FORC distribution $\rho(H_a,H_b)$ at a point P is calculated by fitting a polynomial surface of the form $a_1+a_2H_a+a_3H_a^2+a_4H_b+a_5H_b^2+a_6H_aH_b$ on a local square grid with P at the center [11,12]. The value $-a_6$ is $\rho(H_a,H_b)$ at P. The smoothing factor (SF) sets the size of the local square grid on which the polynomial fit of the magnetization is performed. The number of points on the grid is $(2SF+1)^2$ [11,12]. For example, an SF of 3 means that the smoothing is performed across a $7\times7$ array of data points. Smoothing is necessary in order to reduce the effect of measurement noise that is magnified by the second derivative. We used an SF between 3 and 5 in most cases. Positive regions on the FORC diagram are indicated by a light shading and negative regions by a dark shading.

Under some circumstances, Preisach and FORC diagrams are identical. Néel's interpretation of Preisach diagrams for interacting SD grains is that the $H_c$ coordinate represents the microcoercivity whereas the $H_u$ coordinate represents the interaction field [13].

It has been shown both experimentally and theoretically that particles having different grain sizes and interaction states will plot in different areas of the FORC diagram [11,12,14,15]. Non-interacting

SD grains are characterized by closed contours extending along the $H_c$ axis and with little vertical spread along the $H_u$ axis. PSD grains show a closed-contour distribution that is more spread out along the horizontal axis, with a peak moving toward the $H_u$ axis. For MD grains, the contours broaden along the $H_u$ axis and ultimately form vertical contours. The presence of interactions usually produces a spreading of the distribution in the vertical direction of a FORC diagram. FORC diagrams can also be used to identify the presence of several magnetic minerals in a sample (for example [11,16]).

If the FORC technique is to become widely used, it is important for it to be thoroughly understood. In this paper we use micromagnetic modeling for the first time to predict the theoretical FORC distributions of SD to small PSD grains, as well as arrays of SD particles. In sediments and igneous rocks, the magnetic properties are often controlled by magnetite ($Fe_3O_4$) because of its frequent occurrence and because the magnetization of SD magnetite is stronger than that of other magnetic minerals. This is why we model a magnetite-like mineral. An independent study produced micromagnetic models of FORC diagrams, but for two-dimensional lattices [17]. This is not relevant to rock magnetism but only to thin films.

## 2. Micromagnetic model

We used a three-dimensional unconstrained micromagnetic calculation [18,19] based on the equations formulated by Brown [20]. The algorithm was fully described by Wright et al. [21]. A single particle is modeled by subdividing it into $N = n \times m \times l$ cubic subcells, where $n$, $m$ and $l$ are the numbers of subcubes in the $x$, $y$, and $z$ directions. The magnetization of the subcubes is uniform within each cube and fixed in magnitude but can vary in direction, so we can characterize it with two angles. The domain structure is calculated by using a conjugate gradient (CG) algorithm with a fast Fourier transform to minimize the total magnetic energy, which is the sum of the exchange energy, the magnetostatic energy and the anisotropy energy [19,21]. The minimization gives a local energy minimum.

The resolution of the models is determined by the size of the cell edge, which has to be smaller than half the exchange length $d_{ex} = \sqrt{2C_E/(\mu_0 M_s^2)}$, where $C_E$ is the exchange constant [22]. However, in modeling SD particles, reducing the resolution does not significantly affect the behavior. Moreover, we are not attempting to produce definitive hysteresis curves, but to look at the trends and how they might affect FORC analysis. The room-temperature values of the magnetic constants used are: $M_s = 480$ kA m$^{-1}$ [23], $C_E = 1.3 \times 10^{-11}$ J m$^{-1}$ [24], and $K_1 = -1.25 \times 10^4$ J m$^{-3}$ [25].

The partial hysteresis process is modeled by saturating the grain with an appropriate positive field. The field is then decreased in 2 mT steps until it reaches saturation in a negative field. An equilibrium state is found at each field. FORCs are modeled by starting from each state obtained on the initial descending hysteresis curve and increasing the field back to positive saturation. The field increment is also 2 mT. This increment was chosen so that the total number of FORCs is around 100, a number usually accepted as large enough to obtain a good-quality FORC diagram [11,12]. In order to avoid marginally stable states, we introduce perturbations of 5° or less to each dipole and re-run the minimization until the energy difference between two successive minimizations normalized to the SD energy is less than $10^{-3}$. We tested the effect of varying these two minimization parameters (perturbations between 3 and 8° and energy differences between $10^{-2}$ and $10^{-4}$). The micromagnetic states are not affected by these changes, although the fields at which switching occurs vary between 2 and 4 mT.

The model does not include the effect of thermal fluctuations. Simulated annealing (SA), which imitates the effect of thermal fluctuations in a random, undirected procedure (e.g. [26]), increases computational time by orders of magnitude compared to the directed CG algorithm. The large resolution that is required to model arrays of particles makes it impossible to use SA in our calculations. SA and other pseudo-thermal

perturbation methods generally find somewhat lower energy states than the CG method, but the differences are not large [27], nor are they vital in our application.

As a test of our model, we calculated the hysteresis loop for a thin sheet of permalloy (standard problem #1 from [28]). Our model is not optimized for two-dimensionnal problems, so we used a resolution of $50\times25\times1$ cells smaller than what is ideally required by the exchange length of permalloy. Therefore, we also had to increase the thickness of the permalloy sheet from 20 to 40 nm. Nevertheless, we find a coercivity of 4.1 mT when the external field is applied along the short axis of the sheet (Fig. 1), which is consistent with some of the submitted solutions for this problem (e.g. ts96b, $H_c = 5.3$ mT; pb97, $H_c = 4.9$ mT [29]).

In cases where we modeled an elongated grain, we did not include magnetocrystalline anisotropy energy. If the elongation $q$ exceeds 1.1, the shape anisotropy will dominate over the magnetocrystalline anisotropy.

We also omit magnetostrictive energy because it does not have a significant effect on the domain structure for particles smaller than $\sim$4 μm [30]. The particles modeled in this study are defect-free and stress-free, so we did not include magnetoelastic energy in the model.

It is important to note that a number of simplifications have been made in the model to make the computation feasible. We have neglected thermal fluctuations and any mineral microstructure, and have assumed a very simple grain geometry. Our goal in this study is to examine the trends of hysteresis properties and we make no claim that the coercivities or remanences would be a good match for realistic grain geometries. What is intended is that some insight should be gained as to the effects of grain interactions and domain states on the trends observed in FORC analysis.

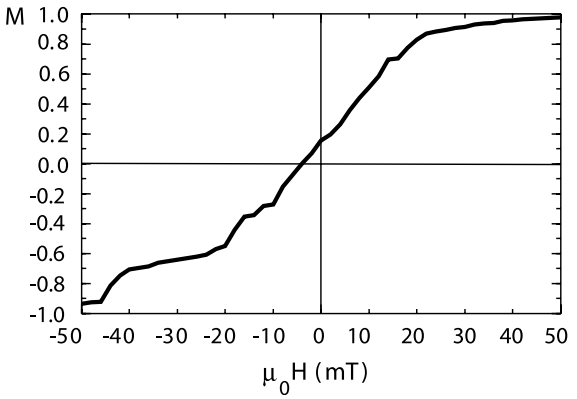


Fig. 1. Half major hysteresis loop for our solution to the permalloy thin sheet micromagnetic problem #1 from [28]. The field is along the short axis of the sheet.

## 3. Hysteresis and FORC diagrams of isolated grains as a function of size

### 3.1. Single field orientation

In an elongated grain of magnetite, the easy axis of magnetization is along the direction of elongation and the hard axes are along two directions perpendicular to the easy axis. It is considerably more difficult to saturate the magnetization of a magnetite crystal along the hard direction than along the easy direction, and therefore we expect the hysteresis curves and the FORC diagrams to be different depending on the field orientation.

Micromagnetically calculated FORC diagrams are shown in Fig. 2 for an SD particle with the field applied along an easy axis, a hard axis, and an intermediate direction. The particle size is $0.045\times0.03\times0.03$ μm, i.e. an elongation ratio of 1.5.

We obtained rectangular hysteresis loops for SD particles if the field was applied along the easy axis. If the field was applied along the hard axis, the magnetization rotated reversibly at all fields. In both cases, the magnetization reversed by coherent rotation. This behavior is consistent with results from other studies [31–33]. If the field was applied at nearly 45° to the easy axis, the hysteresis showed a combination of reversible and irreversible behavior. The coercive force in this case was approximately half the coercive force for the field along the easy axis, as predicted by Stoner and Wohlfarth [34].

In the two cases where there is hysteresis, ideally the FORC diagram would display a delta peak at the coercive field $H_c$ with no spread in the

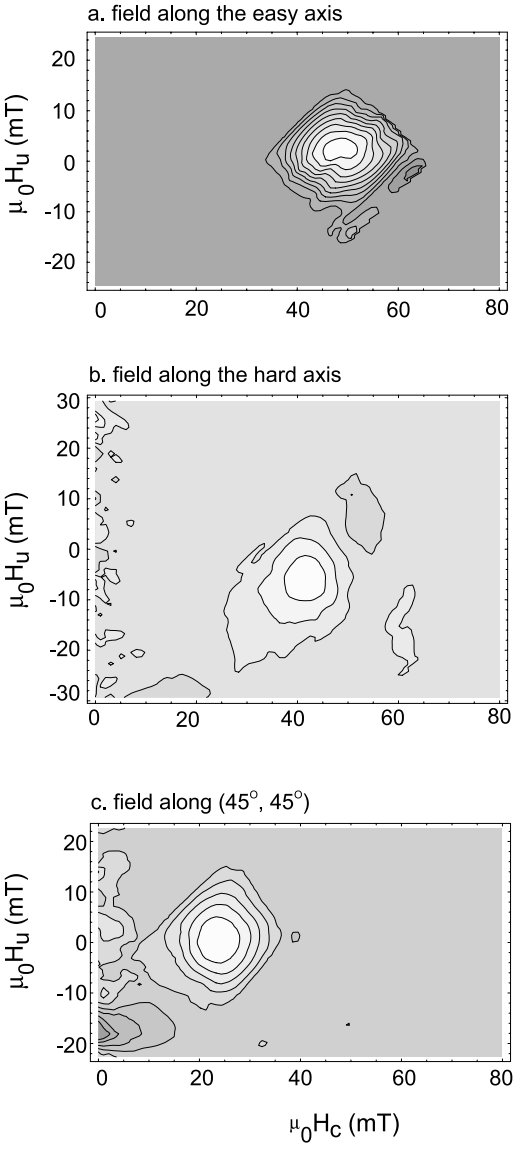


Fig. 2. FORC diagrams for an isolated elongated SD grain (grain size 0.045×0.03×0.03 μm, elongation ratio 1.5). (a) Field oriented along the easy axis; (b) field oriented along the hard axis; (c) field oriented at 45° to the easy axis axis. SF = 5.

$H_u$ direction (zero interaction field in the Preisach–Néel interpretation). In reality, the peak has a finite width due to the fitting of a polynomial function and to the spread of coercivities on the reversal loops caused by perturbations introduced in the minimization process [12] (2–4 mT). For all the following models of isolated particles, we use the intermediate field orientation at 45° to the easy axis.

When the grain size is increased just above the SD–PSD limit to a 0.10×0.08×0.08 μm grain ($q = 1.25$), the magnetization reverses during the major hysteresis loop through a vortex state which is stable for applied fields between −10 and −26 mT. Nucleation of the vortex is progressive. The initial state is a flower state (Fig. 3a), i.e. a SD state with fanning of the magnetization from the uniform state near the grain surface. The next state (Fig. 3b) is a precursor to a vortex state, which collapses to a well-defined vortex state on relaxation of the applied field (Fig. 3c). Such behavior has been described by Enkin et al. [35] while modeling PSD magnetite grains. The vortex exits at one of the corners through the same intermediate state previously described (Fig. 3d) and the structure becomes a flower state in the negative saturation field (Fig. 3e).

Secondary branches appear in the reversal curves when the fields are in the range of any of the intermediate states between the two flower states (Fig. 4a) [36]. This causes the main peak on the FORC diagram to split into several positive and negative peaks (Fig. 4b).

Although we tried to minimize instabilities as much as possible, switching to a vortex state or to a flower state does not occur at exactly the same field for all the reversal curves. In some cases, the micromagnetic state does not pass through the vortex state and flips directly to the flower state. As a result, smaller secondary peaks appear on the FORC diagram and the peaks are relatively spread out (Fig. 4b). The ∼45° line of alternating positive and negative peaks is due to the perturbations introduced in the model to test the stability: this causes the Barkhausen jumps to occur at different fields on each reversal curve. The same pattern has been observed by C.R. Pike (personal communication) in pyrrhotite single grains.

For a somewhat larger grain (0.12×0.09×0.09 μm), the intermediate states encountered during the magnetization reversal are more numerous and complex, leading to a large number of different reversal curves and peaks on the FORC diagram.

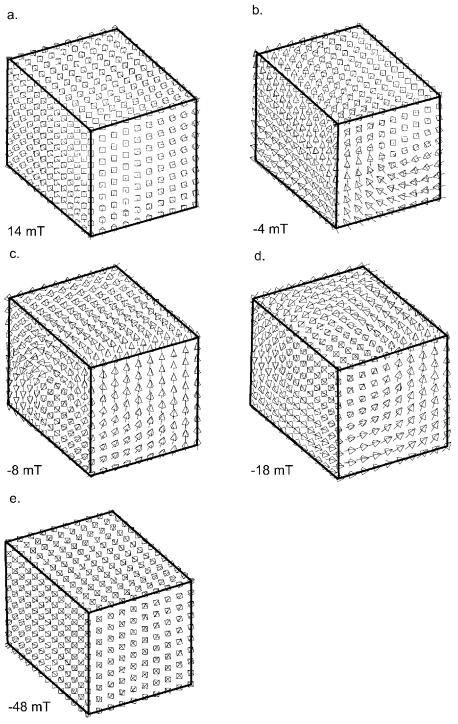


Fig. 3. Micromagnetic structure obtained during a complete hysteresis loop for a $0.10\times0.08\times0.08$ μm isolated particle. (a) Applied field is 14 mT; (b) applied field is −4 mT; (c) applied field is −8 mT; (d) applied field is −18 mT; (e) applied field is −48 mT. Arrows represented by a cross inside a square are pointing out of the page; arrows with a dot inside a square are pointing into the page.

### 3.2. SD grains oriented in different directions

In order to reproduce the distribution of orientations of the grains in a natural sample, we averaged FORC distributions for a set of 200 random field orientations. The particle size is $0.045\times0.03\times0.03$ μm. The FORC distribution is now more spread out on the $H_c$ axis than on the $H_u$ axis (Fig. 5). We would expect the FORC diagram to be elongated along the $H_c$ axis because particles with different orientations have different coercive fields. Again, the spread on the interaction axis is due to the averaging effect of the SF and to the perturbations introduced during the minimization process. The 'boomerang shape' may be an effect of different return paths of the FORCs. If $H_a$ is a saturating field, then the FORCs are identical. However, if $H_a$ is not a saturating field, then the return curves for randomly oriented grains display a dependence on $H_a$ at relatively large positive fields.

## 4. Hysteresis and FORC diagrams of three-dimensional arrays: effect of interactions

Three-dimensional arrays of particles were modeled by masking some cells in a model consisting of a large number of cells. In so doing, it was possible to vary the size of the grains in the array as well as the spacing between the grains within the array. Based on micromagnetic calculations, grains interact significantly if the spacing between them is smaller than one grain width [31,37]. Modeling the effects of interactions on magnetic susceptibility in distributions of Stoner–Wohlfarth SD particles, Muxworthy [38] found that the effect of interactions drops off when the spacing between grains is between one and two times the grain diameter. Modeling arrays of particles requires high resolution, so we restricted ourselves to arrays of $2\times2\times2$ and $3\times3\times3$ SD particles. A $2\times2\times2$ array is physically somewhat unrealistic, but it allows us to gain some insight into interaction effects within the constraints of current computational resources.

### 4.1. Arrays of aligned particles

Arrays are formed of elongated particles aligned along the same direction ($z$ axis). The size of each SD particle within the array is $0.045\times0.030\times0.030$ μm ($q=1.5$). The resolution of each individual grain is $3\times2\times2$ cells. The spacing is defined as the distance corresponding to the free space between grains. The field is still oriented at 45° to the easy axis.

#### 4.1.1. $2\times2\times2$ arrays

Hysteresis and reversal curves depend crucially on the spacing between grains. When the spacing between particles is twice the particle length or more, the micromagnetic structure is uniform and evolves toward a flower state as the field is decreased. Magnetic moments are aligned within one grain and with those of other grains. At a

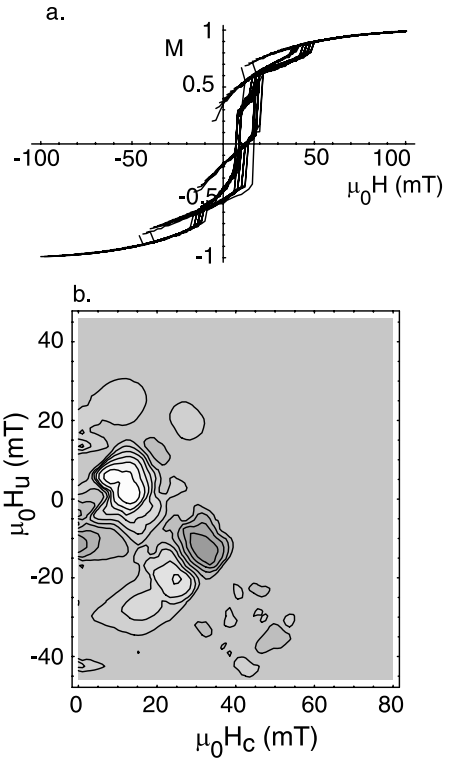


Fig. 4. Hysteresis loop with reversal curves (a) and FORC diagram (b) of an isolated elongated PSD grain (grain size 0.10×0.08×0.08 μm). The field is oriented at 45° to the easy axis. SF = 5.

particular switching field, all the moments rotate coherently, then the structure again evolves toward a flower state where less and less deflection of the spins is observed at the corners as the field intensity increases. The FORC diagram is similar to that observed for a single crystal (Fig. 6a). It has a single peak centered at zero interaction field and at the coercive field of the particle ensemble.

The hysteresis and micromagnetic structure of the array show some specific features when the spacing is reduced (Fig. 6b). First, the hysteresis loop exhibits two jumps when the field is decreased. The micromagnetic structure in the critical region of a reversal curve is shown in Fig. 7. Between saturation and the first switching field, all the grains have a uniform magnetization oriented in the direction of the field. Then, there is an intermediate state (when the field is between 38 and 60 mT) where each grain still has a uniform magnetization, but where half of the grains have reversed their moments. Finally, all the moments switch again to a uniform state.

The presence of these two switching fields causes the hysteresis curve to show two discontinuities, as was found also by Virdee [31]. The reversal curves have different behavior depending on the reversal field $H_a$ at which the curve begins. If $H_a$ is larger than the first switching field, the reversal curve follows the same path as the hysteresis curve, and the structure stays as a flower state nearly up to saturation. If $H_a$ is between the two switching fields, the reversal curve shows one jump at which the structure suddenly changes from a vortex state to a flower state, and then stays as a flower state. Finally, if $H_a$ is less than the second switching field, the array undergoes either one or two switching events: the intermediate vortex is not always reached and if it is, only for a narrow range of fields (typically between 4 and 8 mT).

If the spacing is less than two-thirds the particle length, the intermediate state exists for a large range of fields (between 25 and 40 mT). The switching to the intermediate state or to the flower state on the reversal curve happens at almost the same fields for all the different reversal curves (within 2–4 mT). As a result, the FORC diagram shows three distinct peaks corresponding to each switching: one for the switching from intermediate state to the flower state when $H_a$ is in the

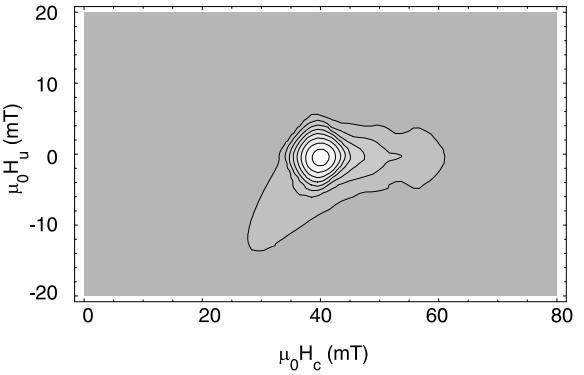


Fig. 5. Average of 100 FORC diagrams of isolated elongated SD grains (grain size 0.045×0.03×0.03 μm, elongation ratio 1.5), with the applied field oriented along 100 different randomly chosen directions. SF = 3.

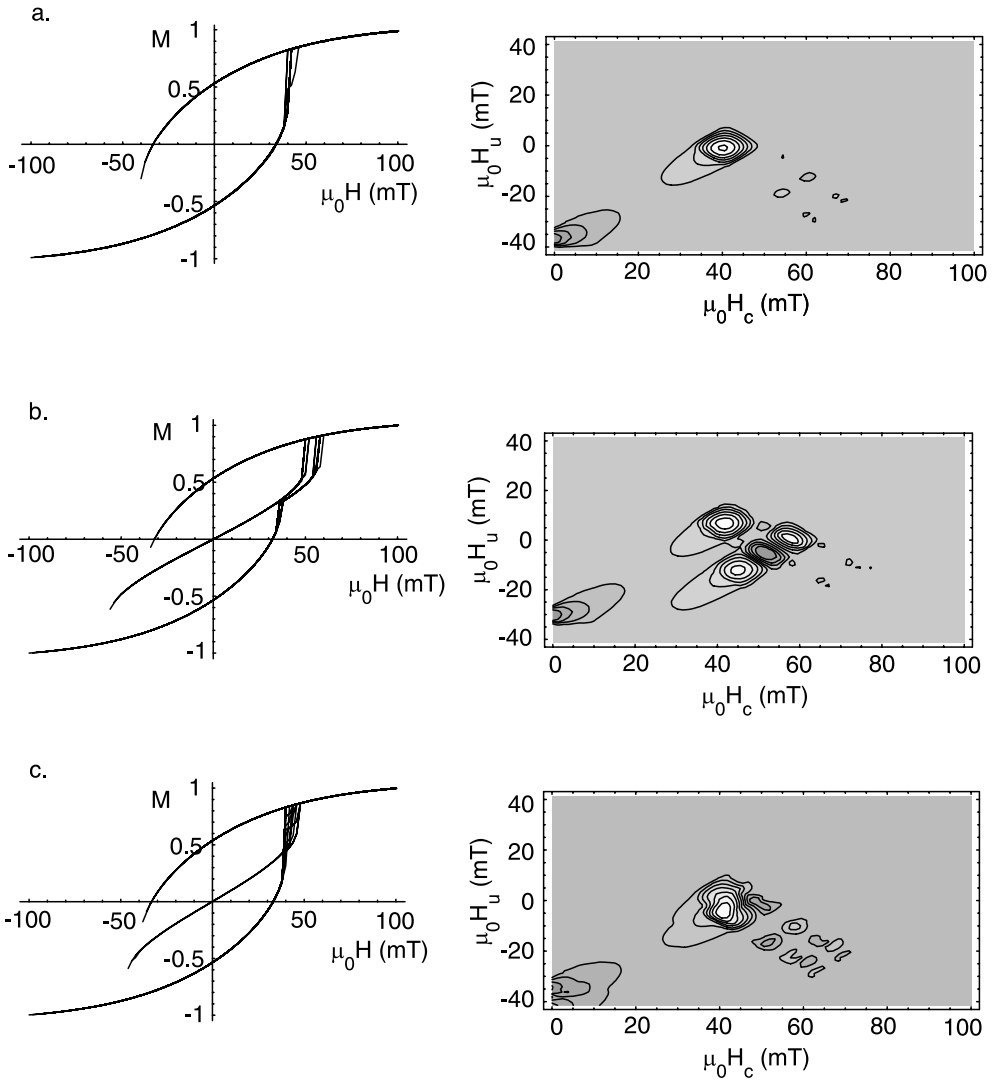


Fig. 6. Hysteresis loops with reversal curves and FORC diagrams for an array of 2×2×2 elongated SD grains (grain size 0.045×0.03×0.03 μm, elongation ratio 1.5). The spacing between the different grains is: (a) twice the grain length; (b) two-thirds the grain length; (c) four-thirds the grain length. SF = 4.

range where the intermediate state is stable; one for the switching from flower state to intermediate state; plus one for the switching from the intermediate state to the flower state when $H_a$ is beyond the range of stability of the intermediate state (Fig. 6b).

The range of stability of the intermediate state decreases when the spacing is increased. When the spacing is between two-thirds and twice the particle length, the intermediate state is only stable for a narrow range of fields: from 12 mT for a spacing of one particle length to 4 mT for a spacing of five-thirds the particle length. The switching does not occur at the same field for the different reversal fields, but over a range of about 8 mT. The two ranges of fields during which switching occurs overlap. This effect causes the peaks on the FORC diagram to appear much more noisy, and to eventually form only one peak (Fig. 6c). With the increasing variation of switching fields de-

pending on the reversal fields we also observe the appearance of a 45° line of alternating positive and negative peaks. When the intermediate state is stable over a range smaller than 4 mT, as is the case for a spacing of five-thirds the particle length, it is possible that the present state would completely disappear when the minimization parameters are changed. In this case, the array would behave as a non-interacting ensemble. For this array the critical spacing for the array to behave as a non-interacting array is between five-thirds and two particle lengths.

The ratio $M_{rs}/M_s$, which is traditionally used as an indicator of particle size, remains fairly constant when the spacing of the grains is changed (Fig. 8a). In particular, there is no obvious variation when the secondary branch disappears as a result of going from an interacting to a non-interacting system. The coercive field $H_c$ is also fairly constant when the spacing of the grains varies (Fig. 8b). In this special grain arrangement, where all the grains are aligned, these two parameters would fail to indicate the interaction state of the system.

The effect of varying the spacing in an array of $2\times2\times2$ grains is shown in Fig. 9. For the irregularly spaced grid, there is a slight variation in coercivity depending on the spacing, but the main features on the FORC diagram are still the same. In general, FORC diagrams for irregular arrays are intermediate between the FORC diagram for equally spaced arrays with separations equal to the largest and smallest separations in the irregular array, respectively.

#### 4.1.2. $3\times3\times3$ array

Now, the model contains 27 elongated SD ($0.045\times0.03\times0.03$ μm) particles, arranged in a

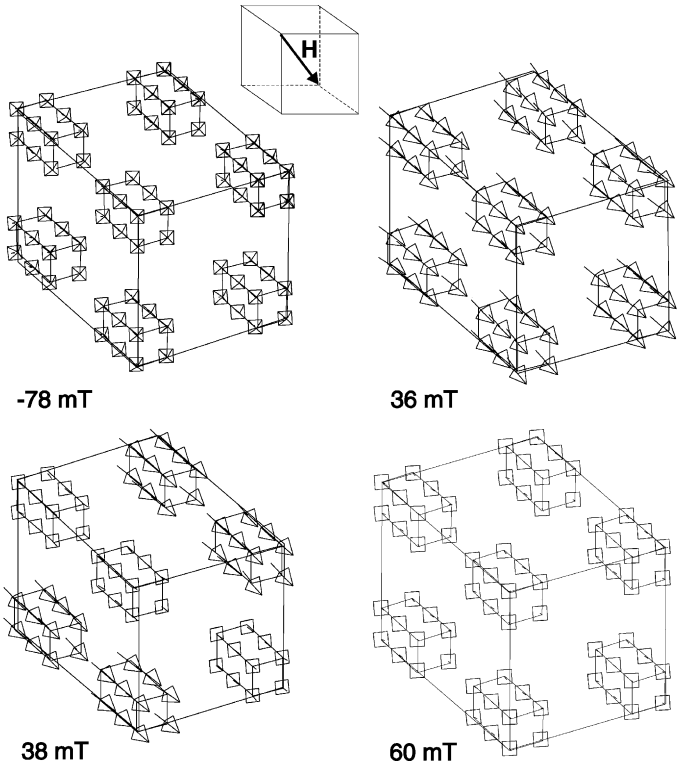


Fig. 7. Micromagnetic structure of an array of $2\times2\times2$ interacting elongated SD grains (grain size $0.045\times0.03\times0.03$ μm, elongation ratio 1.5). The reversal field is −80 mT. (a,b) All the moments are still antiparallel to the field. (c) Half of the moments have reversed. (d) All the moments are aligned with the field. Arrows represented by a cross inside a square are pointing out of the page; arrows with a dot inside a square are pointing into the page.

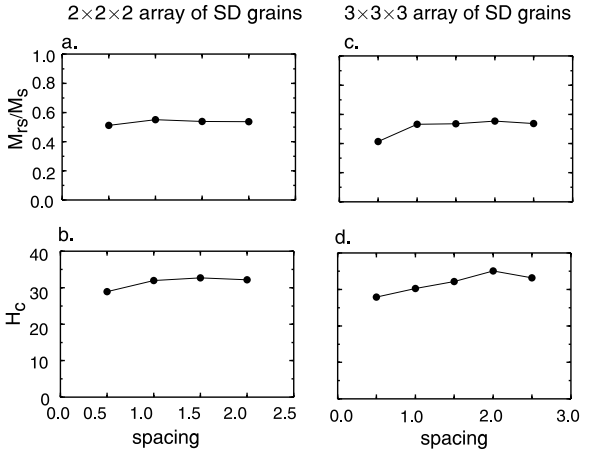


Fig. 8. Hysteresis parameters as a function of spacing between particles for 2×2×2 (a,b) and 3×3×3 (c,d) arrays of elongated aligned SD particles. Spacing is in particle widths.

3×3×3 array. We again found that there is a threshold in the spacing between cells that determines whether the grains are interacting (Fig. 10). The spacing has to be more than twice the grain length in order for the particles to behave like isolated grains (Fig. 10a): all the moments are aligned with the field at saturation, then the structure slowly evolves toward a flower state. All the moments reverse coherently at the same switching field. The reversal curves are either symmetrical with the main loop if the reversal field is smaller than the switching field, or they follow the main loop if the reversal field $H_a$ is larger than the switching field. This behavior results in a single peak on the FORC diagram.

If the spacing between grains is less than twice the grain length, intermediate states appear on the major hysteresis loop, leading to secondary branches on the reversal curves. The intermediate structures are now more complex than for the 2×2×2 array. Each jump in the hysteresis loop and the reversal curves corresponds to one or several of the grains reversing their magnetization, as shown by Pike and Fernandez [14] (Fig. 11). In general, the smaller the spacing, the more secondary branches appear. As for the 2×2×2 array, secondary branches give rise to several peaks on the FORC diagram (Fig. 10b). We can distinguish

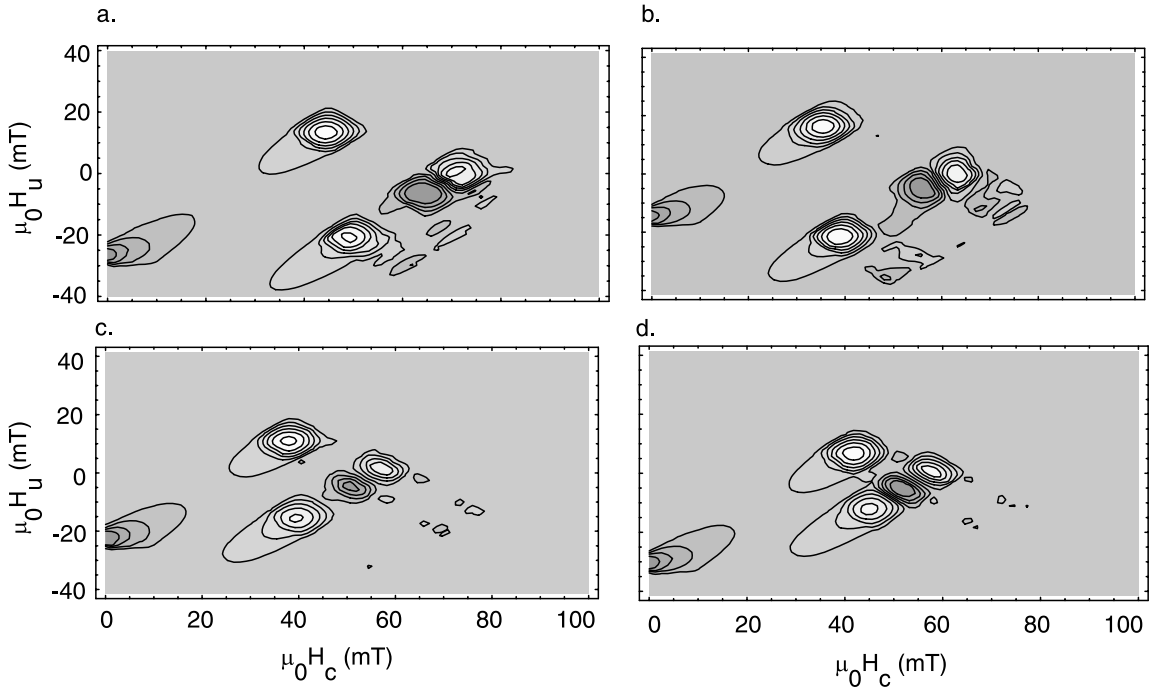


Fig. 9. FORC diagrams for arrays of 2×2×2 particles with different sets of spacings between grains. Spacings between grains in terms of particle length are: (a) 1/3, 1/3, 1/3; (b) 1/3, 1/3, 2/3; (c) 1/3, 2/3, 2/3; (d) 2/3, 2/3, 2/3. SF = 4.

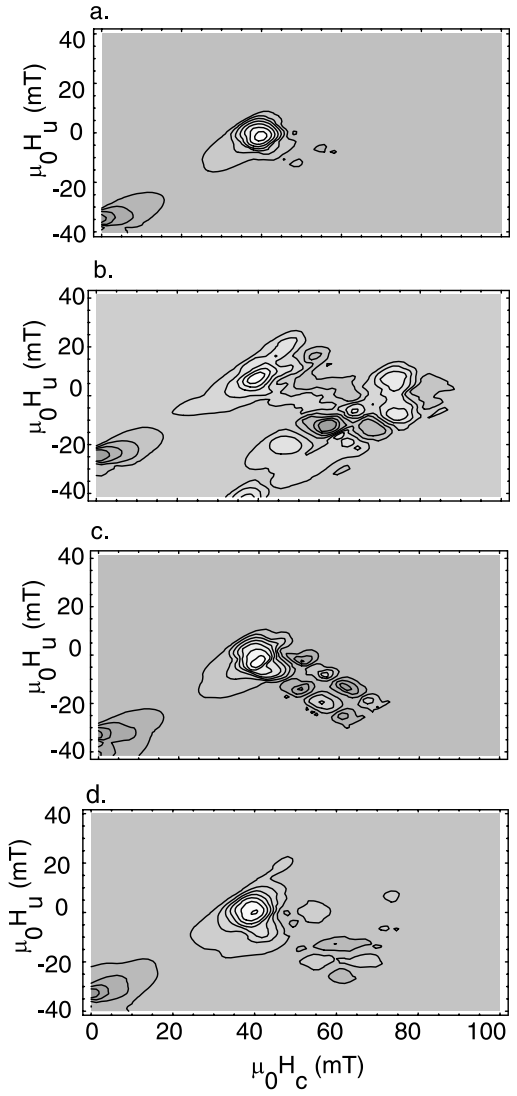


Fig. 10. FORC diagram for an array of 3×3×3 elongated SD grains (grain size 0.045×0.03×0.03 μm, elongation ratio 1.5). The spacing between grains is: (a) 5/3 the grain length; (b) 1/3 the grain length; (c) 4/3 the grain length. (d) Average of FORCs for spacings of 1/3, 2/3, 1 and 4/3 the grain length. SF = 4.

separated peaks up to a spacing of one particle length. When the spacing is between four-thirds and twice the particle length, the switching ranges all overlap on the reversal curves and it becomes difficult to judge if the secondary peaks are due to different switching fields because of different micromagnetic states on the reversal curve or to the range of fields over which switching occurs (Fig. 10c). These ranges are so small that, again, some states can disappear when varying the minimization parameters. In this case, we establish the critical spacing for the array to interact between four-thirds and twice the particle length.

In an attempt to simulate the effects of interactions in a random assemblage of particles in a real sample, we averaged the FORC diagrams obtained for interacting arrays of spacing 1/3, 2/3, 1, and 4/3 the grain length (Fig. 10d). One main peak emerges that is wider on the $H_u$ axis than the peak observed in the non-interacting case (Fig. 10a). This supports the idea that the spread on the $H_u$ axis observed in interacting assemblages in natural samples might be due to a superposition of the secondary peaks we observed on very small arrays.

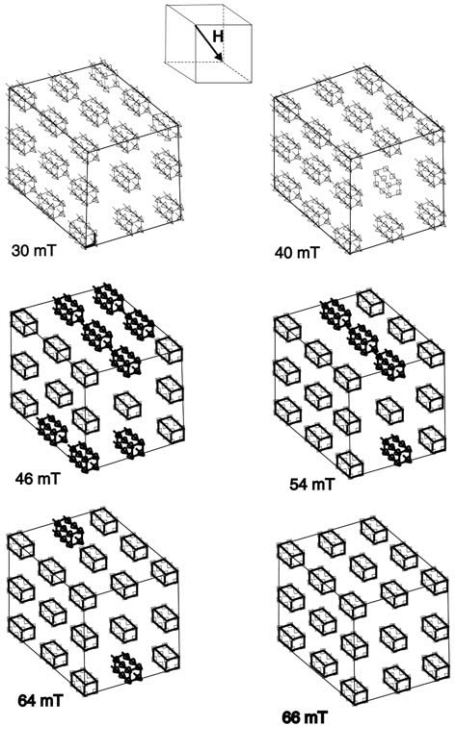


Fig. 11. Micromagnetic structure of an array of 3×3×3 interacting elongated SD grains (grain size 0.045×0.03×0.03 μm, elongation ratio 1.5) during the measurement of a reversal curve corresponding to a reversal field of −70 mT. Arrows represented by a cross inside a square are pointing out of the page; arrows with a dot inside a square are pointing into the page.

The full width at half maximum (FWHM) of the main peak of the cross-section taken in the $H_u$ direction through the maximum of the FORC distribution is a measure of interaction in the Néel model [12]. As expected, it shows a decrease when the spacing is increased (Fig. 12). The first point (measured when the spacing is half the grain width) was not well defined because of the multiple peaks on the FORC diagram.

Again, the ratio $M_{rs}/M_s$ stays constant and could not be used to indicate a change in the interaction state of the system (Fig. 8c). The coercive field $H_c$ increases when the spacing is increased up to two subcells and then decreases slightly (Fig. 8d). However, this variation is not correlated with the change from an interacting to a non-interacting system. In the case of a $3\times3\times2$ or $3\times2\times2$ array, we observed the same pattern as for regular arrays: secondary branches appear as a result of interactions between grains and create secondary peaks on the FORC diagram.

### 4.2. *Array of cubic particles having random magnetocrystalline anisotropy axes*

In order to study the case where particles are randomly oriented within an array, we revert to cubic particles but introduce uniaxial magnetocrystalline anisotropy whose orientation is random. We take for $K_{u1}$ the first magnetocrystalline anisotropy constant for magnetite, $K_1$.

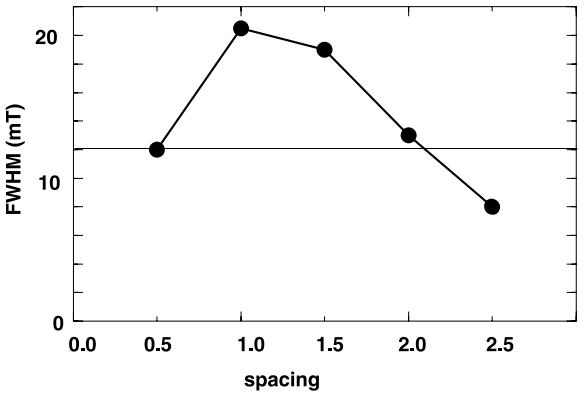


Fig. 12. FWHM of the main peak of the FORC distribution profiled parallel to the $H_u$ axis, as a function of spacing between particles, for a $3\times3\times2$ array of SD elongated particles (grain size $0.045\times0.03\times0.03$ μm). The line at 12 mT represents the FWHM of an individual grain. If there are two peaks on the FORC distribution, we plot the average width of the two peaks. The field is applied at 45° to the easy axis.

In the case of aligned anisotropy axes, the grains behave as a non-interacting array when the spacing is large because they all switch from a flower state in one direction to a flower state in the other direction at the same field. Now each grain has a different anisotropy direction, and so there is a range of switching fields. There are many more intermediate states, in principle one for each grain. There is a similar distribution for switching from the anisotropy easy axis to alignment with the negative field. Thus, the FORC diagram has a multiplicity of peaks. In the interacting case, the ensemble should behave more like a single magnetic structure, with grains reversing their magnetizations in different stages but this time because of the interactions. In both cases there will be intermediate states during the reversal process creating multiple peaks on the FORC diagram, but it is difficult to know if this effect is due to interactions between grains or because the moments of grains orient along different anisotropy axes when the field is reduced. Moreover, FORC diagrams are noisier than in the case of aligned shape anisotropy axes, making it even more difficult to look for fine features that might distinguish between the two cases.

## 5. Discussion

Our FORC diagram for models of isolated SD particles is consistent with Stoner–Wohlfarth theory [34]. FORC diagrams for PSD particles are characterized by secondary peaks resulting from minor branches on the reversal curves.

Our micromagnetic models of FORC diagrams for assemblages of SD grains show distinctive features that can help to differentiate between interacting and non-interacting assemblages. For arrays of SD particles having aligned anisotropy directions, the presence of minor branches on the reversal curves indicates interactions among grains and causes the FORC diagram to have several positive and negative peaks instead of

the single peak that occurs when the grains behave as independent systems. When the particles are closely spaced in a large array, the FORC distribution becomes noisy. In simpler cases (smaller arrays or fewer interacting particles where there is only one minor branch), we can identify two positive peaks that are symmetrical with respect to the $H_c$ axis, another positive peak further away on the $H_c$ axis at $H_u = 0$, and a negative peak between the latter positive peak and the lower positive peak (Fig. 6).

In order to investigate the superposition of the peaks that would lead to the spread on the $H_u$ axis that is observed experimentally, we modeled an array of $5\times5\times5$ cubic SD particles. Each grain is represented by only one subcube, so the particles are ideal SD. This simplification allows us to compare FORC diagrams for different spacings. The spreading clearly appears in the more interacting array and diminishes with increasing spacing (Fig. 13). Together with the averaging of the four interacting arrays shown in Fig. 10d, this model demonstrates that the superposition of split peaks can explain the spread on the $H_u$ axis.

Pike and Fernandez [14] measured FORC diagrams for an array of Co dots with a strong uniaxial shape anisotropy. When saturated along their short axes, the grains relax into single vortex states [39]. The FORC diagrams measured on these samples show a 'butterfly' structure composed of two positive and two negative peaks. It is difficult to tell if this array is interacting or not because the $M_s$ and $C_E$ for cobalt are three times larger than $M_s$ and $C_E$ for magnetite, the exchange length for cobalt is a hundred times smaller than the exchange length for magnetite, and the anisotropy is crucial for interactions. Therefore, the conclusions drawn from our modeling cannot be quantitatively applied to the observations of Pike and Fernandez [14]. Since we have shown that interactions in arrays of particles with aligned anisotropy axes give rise to multiple peaks on the FORC diagram, it is, however, a possibility that the peaks defining the 'butterfly' structure are due to interactions among grains.

An isolated PSD grain and an array of interacting SD grains show the same features on a FORC diagram, even though the physical origin of the splitting into several peaks is different in the two cases. This ambiguity cannot be resolved by our simple models of identical, regularly spaced grains. In a real sample having a distribution of grain sizes, orientations and spacings, the situation will be different. Experimentally, the FORC distribution of an ensemble of interacting SD grains has a closed peak [11,12,15] that spreads out along the $H_c$ axis because of the distribution of coercivities and in the $H_u$ direction because of the superposition of the secondary peaks caused by interactions. FORC distributions for PSD or MD grains are characterized by contours that di-

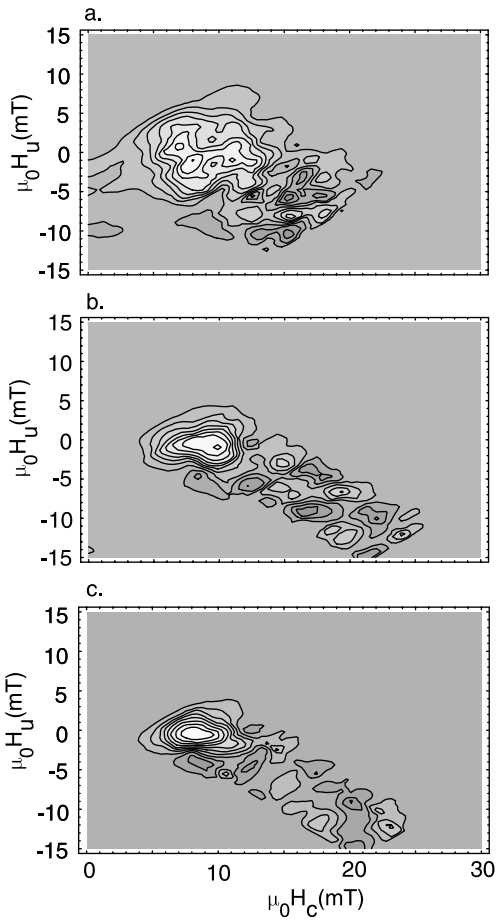


Fig. 13. FORC diagram for an array of $5\times5\times5$ cubic SD particles (grain size 0.04 μm). The spacing between grains is: (a) twice the grain length; (b) three times the grain length; (c) four times the grain length. SF = 5.

verge as one approaches the origin of the diagram [11,15,40]. We can explain the spreading parallel to the $H_u$ axis as a superposition of secondary peaks resulting from the presence of vortex and flower states.

The particles we have modeled are stress-free and defect-free. In real samples, the presence of defects is likely to cause stress fields impeding rotation of SD moments, therefore increasing $H_c$ [41]. The spacing limit between interacting and non-interacting systems may change as well, but the splitting of the peaks would still be observed for interacting arrays.

Measured FORC diagrams are often found to be asymmetrical [11,12,15,42]. Experimental Preisach diagrams are also often asymmetrical [43], even though in theory Preisach distributions are constrained to be symmetrical. The moving Preisach model [43] in which the effective field is the sum of the applied field plus an interaction field proportional to the overall magnetization accounts for most of the asymmetry in Preisach diagrams. We find, however, that FORC diagrams for isolated PSD grains are asymmetrical, as are FORC diagrams for arrays of interacting SD particles.

For some paleomagnetic measurements, such as Thellier–Thellier paleointensity determinations, it is important to know if the assemblage is interacting or not, since interacting assemblages are likely to fail the experiment. The best material for paleointensity experiments should have a FORC diagram with a symmetrical single peak having a high $H_c$ and little spread in the $H_u$ direction. PSD-like FORC diagrams (peak at a smaller $H_c$ and contours converging away from the $H_u$ axis) may also be acceptable.

In paleoclimatic studies, changes in magnetic grain size and mineralogy can indicate changes in magnetic mineral sources and pathways, as well as changes in the flux of magnetic components to the sediment. These changes can be controlled by the effect of climate on the pathways, in particular through changes in atmospheric circulation and ocean currents in the case of deep-sea sediments [1]. In environmental studies, a knowledge of grain size and magnetic mineralogy can give indications on various parameters such as sediment load and velocity, or particle transport during erosion. The ability of FORC diagrams to give a better description of grain size distribution and magnetic mineralogy is therefore also helpful for environmental and paleoclimatic studies.

## 6. Conclusions

We carried out micromagnetic modeling of FORC diagrams. Isolated elongated SD particles show a single positive peak centered at $H_c, H_u = 0$. Isolated elongated PSD particles have complex FORC distributions with several secondary positive and negative peaks, caused by intermediate vortex structures.

Arrays of interacting SD particles with aligned uniaxial shape anisotropy also display several peaks on the FORC distribution caused by the existence of one or several minor branches on the reversal curves. Arrays of non-interacting particles do not show these peaks but only a single peak centered at zero on the $H_u$ axis and at the average coercive field of the assemblage on the $H_c$ axis. Splitting of the central peak on the $H_u$ axis when particles begin interacting might explain the vertical spread observed on FORC diagrams of natural interacting samples as an effect of superposition of multiple peaks due to the random orientation of a large number of grains. We did not observe any significant changes in the usual hysteresis parameters $M_{rs}/M_s$ and $H_c$ that would indicate the interaction state. In the case of arrays of SD particles with aligned uniaxial anisotropy, the presence of multiple peaks on the FORC diagram is a much better indicator of interactions than variations in hysteresis parameters.

The presence of multiple peaks could be a manifestation of intermediate vortex structures in PSD grains as well as of interactions in arrays. In a real sample where anisotropy axes are different for each grain and where grains have a distribution of coercivities, the effects of PSD grains will be different from the effects of interactions. According to our model, we suggest that the spread observed on the $H_u$ axis in natural samples with interactions is caused by the superposition of split peaks.

## Acknowledgements

We thank Chris Pike for providing the FORC analysis software and for his help, and Andrew Newell, Andrew Roberts, Kenneth Verosub and Lisa Tauxe for helpful discussions. The paper was substantially improved by critical reviews from Mark Dekkers, Chris Pike, Andrew Roberts and Michael Winklhofer. This research has been supported by NSERC Canada Grant A7709 to D.J.D. *[RV]*

## References

[1] R. Thompson, F. Oldfield, Environmental Magnetism, Allen and Unwin, London, 1986.
[2] K. Fabian, A. Kirchner, W. Williams, F. Heider, T. Leibl, A. Hubert, Three-dimensional micromagnetic calculations for magnetite using FFT, Geophys. J. Int. 124 (1996) 89–104.
[3] E. Thellier, O. Thellier, Sur l'intensité du champ magnétique terrestre dans le passé historique et geologique, Ann. Géophys. 15 (1959) 285–376.
[4] S. Levi, R.T. Merrill, Properties of single-domain, pseudo-single domain and multidomain magnetite, J. Geophys. Res. 83 (1978) 309–323.
[5] D.J. Dunlop, G.F. West, An experimental evaluation of single domain theories, Rev. Geophys. 7 (1969) 709–757.
[6] R. Day, M. Fuller, V.A. Schmidt, Hysteresis properties of titanomagnetites: grain size and compositional dependence, Phys. Earth Planet. Inter. 13 (1977) 260–267.
[7] D.J. Dunlop, Theory and application of the Day plot ($M_{rs}/M_s$ versus $H_{cr}/H_c$) 1. Theoretical curves and tests using titanomagnetite data, J. Geophys. Res. B 107 (2002) 2056, doi: 10.1029/2001JB00486, EPM 4-1 to 4-22.
[8] D.J. Dunlop, Theory and application of the Day plot ($M_{rs}/M_s$ versus $H_{cr}/H_c$) 2. Application to data for rocks, sediments and soils, J. Geophys. Res. B 107 (2002) 2057, doi: 10.1029/2001JB00487, EPM 5-1 to 5-15.
[9] O. Henkel, Remanenzverhalten und Wechselwirkungen in hartmagnetischen Teilchenkollectiven, Phys. Stat. Sol. 7 (1964) 919–924.
[10] R.B. Proksch, B.M. Moskowitz, Interactions between single domain particles, J. Appl. Phys. 75 (1994) 5894–5896.
[11] A.P. Roberts, C.R. Pike, K.L. Verosub, First-order reversal curve diagrams: A new tool for characterizing the magnetic properties of natural samples, J. Geophys. Res. 105 (2000) 28461–28475.
[12] C.R. Pike, A.P. Roberts, K.L. Verosub, Characterizing interactions in fine magnetic particle systems using first order reversal curves, J. Appl. Phys. 85 (1999) 6660–6667.
[13] L. Néel, Remarques sur la théorie des propriétés magnétiques des substances dures, Appl. Sci. Res. B4 (1954) 13–24.
[14] C.R. Pike, A. Fernandez, An investigation of magnetic reversal in submicron-scale Co dots using first order reversal curve diagrams, J. Appl. Phys. 85 (1999) 6668–6676.
[15] A.R. Muxworthy, D.J. Dunlop, First-order reversal curve (FORC) diagrams for pseudo-single-domain magnetites at high temperature, Earth Planet. Sci. Lett. 203 (2002) 369–382.
[16] I.H.M. Van Oorschot, M.J. Dekkers, P. Havlicek, Selective dissolution of magnetic iron oxides with the acid-ammonium technique-II. Natural loess and palaeosol samples, Geophys. J. Int. 149 (2002) 106–117.
[17] A. Stancu, C. Pike, L. Stoleriu, P. Postolache, D. Cimpoesu, Micromagnetic and Preisach analysis of the First Order Reversal Curves (FORC) diagram, J. Appl. Phys. 93 (2003) 6620–6622.
[18] M.E. Schabes, H.N. Bertram, Magnetisation processes in ferromagnetic cubes, J. Appl. Phys. 64 (1988) 1347–1357.
[19] W. Williams, D.J. Dunlop, Three-dimensional micromagnetic modelling of ferromagnetic domain structure, Nature 377 (1989) 634–637.
[20] W.F. Brown Jr., Micromagnetics, Wiley, New York, 1963.
[21] T.M. Wright, W. Williams, D.J. Dunlop, An improved algorithm for micromagnetics, J. Geophys. Res. 10 (1997) 12085–12094.
[22] W. Rave, K. Fabian, A. Hubert, The magnetic states of small cubic magnetic particles with uniaxial anisotropy, J. Magn. Magn. Mater. 190 (1998) 332–348.
[23] R. Pauthenet, L. Bochirol, Aimantation spontanée des ferrites, J. Phys. Rad. 12 (1951) 249–251.
[24] F. Heider, W. Williams, Note on temperature dependence of exchange constant in magnetite, Geophys. Res. Lett. 15 (1988) 184–187.
[25] E.J. Fletcher, W. O'Reilly, Contribution of $Fe^{2+}$ ions to the magnetocrystalline anisotropy constant $K_1$ of $Fe_{3-x}Ti_xO_4$ ($0 < x < 0.1$), J. Phys. C Sol. Stat. Phys. 7 (1974) 171–178.
[26] L.C. Thomson, R.J. Enkin, W. Williams, Simulated annealing of three dimensional micromagnetic structures and simulated thermoremanent magnetization, J. Geophys. Res. 99 (1994) 603–606.
[27] L.C. Thomson, A three-dimensional micromagnetic investigation of the magnetic properties and structures of magnetite, Ph.D. Thesis, University of Edinburgh, 1993.
[28] http://www.ctcms.nist.gov/~rdm/mumag.org.html.
[29] http://www.ctcms.nist.gov/~rdm/std1/prob1report.html.
[30] A.R. Muxworthy, W. Williams, Micromagnetic models of pseudo-single domain grains of magnetite near the Verwey transition, J. Geophys. Res. 104 (1999) 29203–29218.
[31] D. Virdee, The influence of magnetostatic interactions on the magnetic properties of magnetite, Ph.D. Thesis, University of Edinburgh, 1999.
[32] W. Williams, D.J. Dunlop, Simulation of magnetic hyste-

resis in pseudo-single-domain grains of magnetite, J. Geophys. Res. 100 (1995) 3859–3871.
[33] W. Williams, T.M. Wright, High resolution micromagnetic models of fine grains of magnetite, J. Geophys. Res. 99 (1997) 30537–30550.
[34] E.C. Stoner, E.P. Wohlfarth, A mechanism of magnetic hysteresis in heterogeneous alloys, Philos. Trans. R. Soc. Lond. 240 (1948) 599–642.
[35] R.J. Enkin, W. Williams, Three-dimensional micromagnetic analysis of stability in fine magnetic grains, J. Geophys. Res. 99 (1994) 611–618.
[36] A.J. Newell, R.T. Merrill, Size dependence of hysteresis properties of small pseudo-single-domain grains, J. Geophys. Res 105 (2000) 19393–19403.
[37] Muxworthy, W. Williams, D. Virdee, The effect of magnetostatic interactions on the hysteresis parameters of single-domain and pseudo-single domain grains, submitted to J. Geophys. Res.
[38] A.R. Muxworthy, Effect of grain interactions on the frequency dependence of magnetic susceptibility, Geophys. J. Int. 144 (2001) 441–447.
[39] A. Fernandez, M.R. Gibbons, M.A. Wall, C.J. Cerjan, Magnetic domain structure and magnetization reversal in submicron-scale Co dots, J. Magn. Magn. Mater. 190 (1998) 71–80.
[40] C.R. Pike, A.P. Roberts, M.J. Dekkers, K.L. Verosub, An investigation of multi-domain hysteresis mechanisms using FORC diagrams, Phys. Earth Planet. Inter. 126 (2001) 11–25.
[41] S. Xu, R.T. Merrill, Microstress and microcoercivity in multidomain grains, J. Geophys. Res. 94 (1989) 10627–10636.
[42] C.R. Pike, A.P. Roberts, K.L. Verosub, FORC diagrams and thermal relaxation effects in magnetic particles, Geophys. J. Int. 145 (2001) 721–730.
[43] P. Hejda, T. Zelinka, Modeling of hysteresis processes in magnetic rock samples using the Preisach diagram, Phys. Earth Planet. Inter. 63 (1990) 32–40.